

Dalton Transactions

Accepted Manuscript



This is an *Accepted Manuscript*, which has been through the Royal Society of Chemistry peer review process and has been accepted for publication.

Accepted Manuscripts are published online shortly after acceptance, before technical editing, formatting and proof reading. Using this free service, authors can make their results available to the community, in citable form, before we publish the edited article. We will replace this *Accepted Manuscript* with the edited and formatted *Advance Article* as soon as it is available.

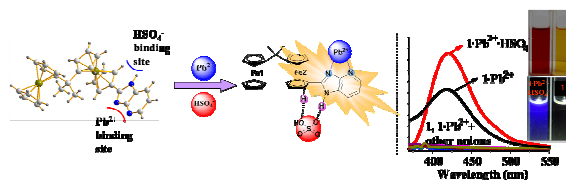
You can find more information about *Accepted Manuscripts* in the [Information for Authors](#).

Please note that technical editing may introduce minor changes to the text and/or graphics, which may alter content. The journal's standard [Terms & Conditions](#) and the [Ethical guidelines](#) still apply. In no event shall the Royal Society of Chemistry be held responsible for any errors or omissions in this *Accepted Manuscript* or any consequences arising from the use of any information it contains.

Graphical abstract

A Simple and Highly Selective 2,2-diferrocenylpropane-based Multi-channel Ion
Pair Receptor for Pb^{2+} and HSO_4^-

Qian Wan^a, Ji-Bin Zhuo^a, Xiao-Xue Wang^a, Cai-Xia Lin^{a,*} and Yao-Feng Yuan^{a,b,**}



2,2-diferrocenylpropane-based multi-channel ion pair receptor **1** was designed and structurally characterized. It was a “naked-eyes-detectable” chemosensor towards Pb^{2+} and HSO_4^- with excellent selectivity and sensitivity.

A Simple and Highly Selective 2,2-diferrocenylpropane-based Multi-channel Ion Pair Receptor for Pb^{2+} and HSO_4^-

Qian Wan^a, Ji-Bin Zhuo^a, Xiao-Xue Wang^a, Cai-Xia Lin^{a,*} and Yao-Feng Yuan^{a,b,**}

Abstract:

Structurally simple, 2,2-diferrocenylpropane-based ion pair receptor **1** was synthesized and characterized by ^1H NMR, ^{13}C NMR, HRMS, elemental analyses, and single-crystal X-ray diffraction. The ion pair receptor **1** showed excellent selectivity and sensitivity towards Pb^{2+} with multi-channel responses: fluorescence enhancement (more than 42-fold), a notable color change from yellow to red, redox anodic shift ($\Delta E_{1/2} = 151$ mV), while HSO_4^- promoted the fluorescence enhancement when Pb^{2+} or Zn^{2+} were bounded to the cation binding-site. ^1H NMR titration and density functional theory were carried out to reveal the sensing mechanism based on photo-induced electron transfer (PET).

1. Introduction

Ion pair recognition is an emerging field of research in supramolecular chemistry, since ion pair receptors are capable of binding concurrently both a cation and an anion and often display higher selectivity and affinity for specific ion pairs than mono-topic receptors able of recognizing a cation or an anion only.¹⁻³ So far, most reported ion pair receptors are constructed on the basis of heteroditopic system,⁴⁻⁵ which is consist of one cation binding domain such as crown ethers,⁶ calixarenes⁷ and one anion binding site for instance pyrrole,⁸⁻⁹ indole, urea,¹⁰ amide,¹¹⁻¹² etc. Recently, it has been found that imidazole is capable of binding both a cation and an anion because it has basic nitrogen as well as acidic -NH group, which converts the imidazole derivatives into excellent ion pair receptors.¹³⁻¹⁷ Terpyridylimidazole ligand reported by Baitalik and coworkers was an effective triple-channel sensor for both Fe^{2+} and F^- ions in solution.¹⁸ Molina and coworkers reported that ferrocene-imidazopyrene dyad behaved as a host-separated ion pair receptor able of recognizing Hg^{2+} and H_2PO_4^- concurrently.¹⁹

Ferrocene is a persistent interest for researchers for it playing a key role as a remarkable redox-signaling. In recent years, mono-core ferrocene and its derivatives have been revealed to be very convenient building blocks for redox-active receptors used for cations and anions recognition.²⁰⁻²⁶ For example, Molina and co-workers reported a ferrocene-based ion pair receptor that only recognized HSO_4^- anion in the presence of Pb^{2+} or Zn^{2+} , whereas no affinity of the free receptor by HSO_4^- anion is observed.²⁷ However, since ferrocene is a known fluorescence quenching group, receptors based on multi-core ferrocene recognizing ions by fluorescence enhancement have been rarely reported.²⁸⁻³⁰ 2,2-Diferrocenylpropane

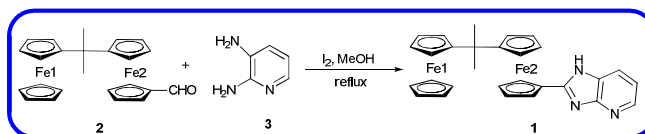
(DFP), readily synthesized from ferrocene and acetone, is one of the most important building blocks for the preparation of multi-ferrocenyl derivatives. DFP has always attracted interest for its unique electrochemical property and present potential applications in anion recognition and catalyzing the decomposition of ammonium perchlorate.³¹⁻³³ Very recently, our group has reported a multi-responsive ion receptor based on DFP and imidazole.³⁴ A multi-channel receptor may display excellent selectivity and sensitivity for specific ion with chromogenic, fluorogenic and electrochemical responsive.^{2, 35-37} As far as we know, the development of multi-channel chromogenic, fluorogenic and electrochemical ion pair receptor utilizing DFP as a building block is still an unreported subject.

Herein, we demonstrated the synthesis, characterization and binding properties of one ion pair receptor **1** consist of DFP and deazapurine, which exhibited enhancement of the fluorescence in the presence of HSO_4^- when Pb^{2+} or Zn^{2+} were bounded to the cation binding-site. Based on the evolution of ^1H NMR titration and density functional theory, it can be speculated that Pb^{2+} and HSO_4^- were combined to receptor **1** in different ways.

2. Results and discussion

2.1. Synthesis and characterization

The receptor **1** was prepared from formyl 2,2-diferrocenylpropane **2**³⁴ and 2,3-diaminopyridine (Scheme 1). The structure of **1** was characterized by ^1H NMR, ^{13}C NMR, HRMS, element analysis and X-ray diffraction. The single crystal of **1** was obtained by recrystallizing from its DMSO solution in a NMR tube. The molecule of **1** crystallizes in monoclinic system, space group $P21/n$. The molecule structure of **1** clearly shows a distorted tetrahedral structure of DFP, where two planes of the mono-substituted Cp linked by methylene are almost in mutually vertical position (dihedral angles 85.18°). The 1-deazapurine backbone and the Cp ring (C19-C23) are almost in a same plane (dihedral angles 1.75°), indicating that there is a conjugation among them. The two Cp rings of Fc1 unit are eclipsed (pseudo-torsion angle of C1-Cg-Cg-C6: 5.57°), while the two Cp rings of Fc2 unit are halfway between eclipsed and staggered (pseudo-torsion angle of C14-Cg-Cg-C19: 11.05°).³⁸ It indicates that the 1-deazapurine backbone has a great effect on Fc2 unit than Fc1 unit. Quite interestingly, N1-H32 \cdots O ($d_{\text{NH}\cdots\text{O}} = 1.80 \text{ \AA}$) and C22-H22 \cdots O ($d_{\text{CH}\cdots\text{O}} = 2.45 \text{ \AA}$) intermolecular hydrogen bonds between the receptor **1** and a solvent molecule DMSO are observed. Crystallographic data, bond distances and angles of the structure are summarized in Table S3 and S4.



Scheme 1. Synthesis of receptor **1**

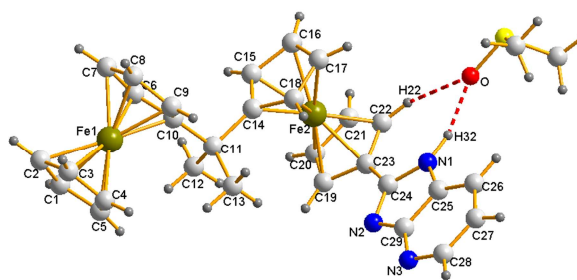


Fig. 1 Intermolecular hydrogen bonds between receptor **1** and solvent molecule DMSO. For more detailed ORTEP view see Figures S4 (significant bond distances and angles in Tables S3, S4).

2.2. Optical response of receptor **1** towards ions

To test its selective detection for cations, the fluorescence spectra of receptor **1** (10 μM) in CH_3CN towards various metallic cations (namely, Na^+ , K^+ , Mg^{2+} , Mn^{2+} , Co^{2+} , Ni^{2+} , Cu^{2+} , Cd^{2+} , Hg^{2+} , Zn^{2+} and Pb^{2+} for perchlorate in aqueous media) were first studied upon excited at 350 nm at room temperature. As shown in Fig. 2, free receptor **1** was weak-emissive, on addition of 5.0 equiv. Pb^{2+} to **1** resulted in a remarkable enhancement of the fluorescence at 420 nm along with a notable color change from yellow to red (Fig. 3). Similarly, Zn^{2+} also induced a little fluorescence enhancement, while other metal ions had little impact on the fluorescence emission. Addition 5.0 equiv. of Pb^{2+} and Zn^{2+} to receptor **1** induced 42- and 11- fold increases in the intensity of spectral changes $(F-F_0)/F_0$, respectively (Fig. S5).

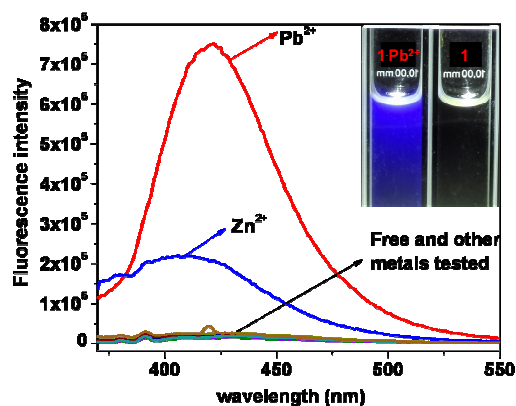


Fig. 2 Fluorescence spectra of **1** (10 μM) in CH_3CN before and after addition of various metal ions, 5.0 equiv. of Pb^{2+} , Zn^{2+} , Mg^{2+} , Mn^{2+} , Co^{2+} , Ni^{2+} , Cu^{2+} , Cd^{2+} , Hg^{2+} , Na^+ and K^+ , excited at 350 nm at room temperature.



Fig. 3 Visual features observed in CH₃CN solutions of **1** (1.0×10^{-3} M) and **1**·Pb²⁺.

The fluorescence titration of **1** (10 μM) by gradually addition of Pb²⁺ (from 0 to 200 μM in H₂O) was comprehensively surveyed. As shown in Fig. 4, a red shift from 390 to 420 nm along with a gradual increase in the intensity of the emission was observed. The red shift may be due to the intra-molecular excimer formation caused by the intermolecular hydrogen bonds between two fluorophores when Pb²⁺ was added.³⁹ In addition, it is pertinent to mention that the increase in fluorescence continued until the addition of 5.0 equiv. Pb²⁺. The fluorescence intensity was proportional to the concentration of Pb²⁺ (from 2 to 40 μM) with a good linear correlation and the minimum detectable amount of Pb²⁺ in this case was calculated to be 4.4×10^{-7} M (0.20 mg L⁻¹) based on S/N = 3,⁴⁰⁻⁴¹ which is lower than the maximum permitted amount of Pb²⁺ (10 mg L⁻¹) in drinking water defined by the World Health Organization.⁴² Job's plot indicated a 1:1 binding stoichiometry for **1** towards Pb²⁺ or Zn²⁺ (Fig. S7 and S8), and the association constant (K_a) of **1** towards Pb²⁺ and Zn²⁺ determined by fluorescence based on the Benesi–Hildebrand method⁴³⁻⁴⁴ were calculated to be 2.11×10^4 M⁻¹ and 1.21×10^5 M⁻¹, respectively (Fig. S9 and S10).

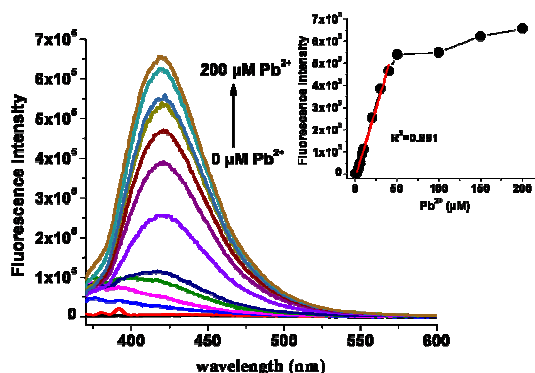


Fig. 4 Fluorescence emission spectra of **1** (10 μM) upon titration with Pb²⁺ (from 0 to 200 μM), excited at 350 nm. Inset: the plot of the fluorescence intensity ($\lambda_{em} = 420$ nm) versus the concentration of Pb²⁺.

Interference experiments on other competitive metal ions to practical applicability of receptor **1** as a Pb²⁺-selective fluorescence receptor were also conducted (Fig. 5). Most of the tested metal ions such as Cd²⁺, Co²⁺, Ni²⁺, K⁺, Mg²⁺, Mn²⁺,

Na^+ and Zn^{2+} had little effect on the fluorescence intensity of **1** with or without Pb^{2+} , but addition of Cu^{2+} or Hg^{2+} induced a slight fluorescence quenching effect. However, compared to receptor **1** toward Cu^{2+} and Hg^{2+} in absence of Pb^{2+} , addition of Cu^{2+} and Hg^{2+} to receptor **1** in presence of 5 equiv. Pb^{2+} induced 32- and 18- fold increases in the intensity of spectral changes, respectively. These results illustrated that **1** still could be a good sensor for Pb^{2+} over various competing metal ions.

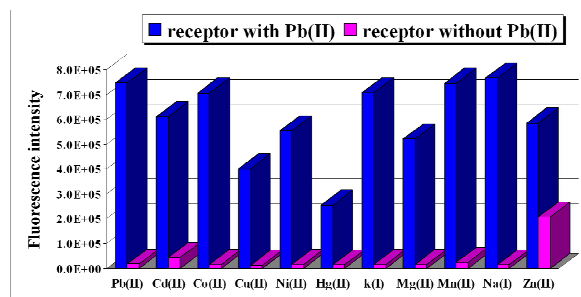


Fig. 5 Fluorescence intensities of **1** (10 μM) in CH_3CN towards 5 equiv. Pb^{2+} and various interferences metal ions (5 equiv.) at 420 nm, excited at 350 nm.

Due to containing an amphoteric imidazole ring in its structure, which is verified an excellent hydrogen bond donor in many anion receptor systems^{29,45}, receptor **1** also has the ability to sense an anion. Thus, on the basis of testing metallic cations, ion pair recognition properties of receptor **1** towards a number of anions were studied. As shown in Fig. 6 and Fig. S11, the fluorescence responses of anions F^- , Cl^- , Br^- , I^- , AcO^- , HSO_4^- , H_2PO_4^- and OH^- in the form of their corresponding tetrabutylammonium salts (TBA^+) to complex $\mathbf{1}\cdot\text{Pb}^{2+}/\mathbf{1}\cdot\text{Zn}^{2+}$ in CH_3CN were investigated. It was worth noting that only HSO_4^- promoted fluorescence enhancement and gave 1.6-fold and 6.6-fold increases in the fluorescence intensity for $\mathbf{1}\cdot\text{Pb}^{2+}$ and $\mathbf{1}\cdot\text{Zn}^{2+}$, while the other anions (F^- , Cl^- , Br^- , I^- , AcO^- , H_2PO_4^- and OH^-) quenched the fluorescence emission of $\mathbf{1}\cdot\text{Pb}^{2+}$ and $\mathbf{1}\cdot\text{Zn}^{2+}$. In addition, HSO_4^- can be very easily distinguished from other anions by the naked eye (Fig. S12) that after the addition of anions except HSO_4^- , the color of the complex $\mathbf{1}\cdot\text{Pb}^{2+}$ changed from red into yellow. The quenching of fluorescence and red-to-yellow color change of complex $\mathbf{1}\cdot\text{Pb}^{2+}$ toward anions F^- , Cl^- , Br^- , I^- , AcO^- , H_2PO_4^- and OH^- maybe ascribed for the dissociation of the complex $\mathbf{1}\cdot\text{Pb}^{2+}$ to $\text{Pb}(\text{X})_2$ and free receptor **1**. Moreover, addition of HSO_4^- and other anions (F^- , Cl^- , Br^- , I^- , AcO^- , H_2PO_4^- and OH^-) to free receptor **1** displayed absolutely no fluorescence enhancement and showed almost no emission in the fluorescence spectra.

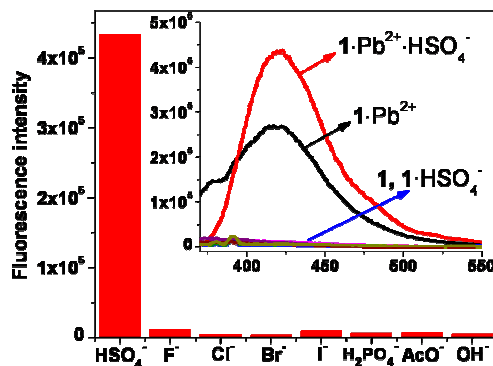


Fig. 6 Emission intensity at 420 nm of complex $1 \cdot \text{Pb}^{2+}$ (10 μM) in the presence of various anions (10 equiv.). Inset: Fluorescence spectra of **1**, $1 \cdot \text{HSO}_4^-$, $1 \cdot \text{Pb}^{2+}$ and $1 \cdot \text{Pb}^{2+}$ with different anions (10 equiv.), excited at 350 nm.

A UV-Visible titration of **1** (25 μM) toward Pb^{2+} (from 0 to 3 equiv.) was performed and analyzed quantitatively. Free receptor **1** displayed the featured $\pi\text{-}\pi^*$ transition band centered at 311 nm ($\epsilon/\text{dm}^3 \text{ mol}^{-1} \text{ cm}^{-1}$ 25 870) and a broad band of lower intensity at 451 nm (1197) attributed to $\text{Fe}^{2+} \rightarrow \text{Cp}$ transition.²² Changes achieved maxima at 1 equiv. of Pb^{2+} , the absorption bands at 311 nm and 451 nm were red shifted to 320 nm and 489 nm, respectively (Fig. 7). Meanwhile, an isosbestic point was observed at 318 nm, indicating that interconversion between two species for **1** after addition of Pb^{2+} was occurred. However, there were no significant changes in the absorption spectra of receptor **1** or complex $1 \cdot \text{Pb}^{2+}$ after addition of HSO_4^- (Fig. S13). Absorption spectra of complex $1 \cdot \text{Pb}^{2+}$ toward other anions such as F^- were also performed and analyzed quantitatively (Fig. S14). We found that F^- can be used as a decomplexation agent for complex $1 \cdot \text{Pb}^{2+}$, which just proved the point that the fluorescence quenching of $1 \cdot \text{Pb}^{2+}$ towards anions X ($X = \text{F}^-, \text{Cl}^-, \text{Br}^-, \text{I}^-, \text{AcO}^-, \text{H}_2\text{PO}_4^-$ and OH^-) were owing to the dissociation of the complex $1 \cdot \text{Pb}^{2+}$ to $\text{Pb}(\text{X})_2$ and free receptor **1**.

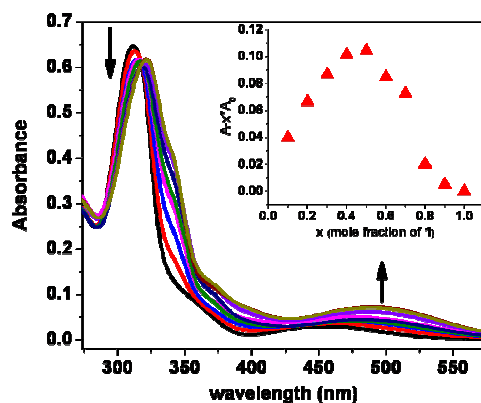


Fig. 7 Absorption spectra of **1** (25 μM) towards Pb^{2+} from 0 to 3 equiv. Inset: Job's plots for the binding of **1** with Pb^{2+} , absorbance at 311 nm.

The electrochemical behaviors of **1** toward various cations above-mentioned were determined by cyclic voltammetry (CV) and differential pulse voltammetry (DPV) in CH_2Cl_2 solutions containing 0.1 M $[(n\text{-Bu})_4\text{N}]\text{ClO}_4$ as supporting electrolyte. As expected, receptor **1** revealed two characteristic reversible redox waves for ferrocene derivatives in CV. The first oxidation wave occurred on Fc1 unit at $E_{1/2} = 469$ mV, then the second redox wave of Fc2 unit emerged at $E_{1/2} = 714$ mV.^{34, 46} On stepwise addition of Pb^{2+} ion up to 1 equiv, a clear anodic shift ($\Delta E_{1/2} = 151$ mV) happened in Fc2 can be observed (Fig. 8), which is owing to the stronger electron withdrawing ability of pyridine after binding with Pb^{2+} . The presence of Zn^{2+} also induced similar shift ($\Delta E_{1/2} = 78$ mV) (Fig. S15), while other metal cations had little effect on either CV or DPV except Cu^{2+} and Hg^{2+} . The accurate test for Cu^{2+} or Hg^{2+} could not be obtained since large precipitation was formed. The precipitation may be due to high reduction potential for $\text{Cu}^{2+}/\text{Cu}^{+47}$ and $\text{Hg}^{2+}/\text{Hg}^+$ in CH_3CN thus Cu^{2+} or Hg^{2+} can act as an oxidant for ferrocene derivatives, which may be the cause of slight fluorescence quenching in interference experiments.

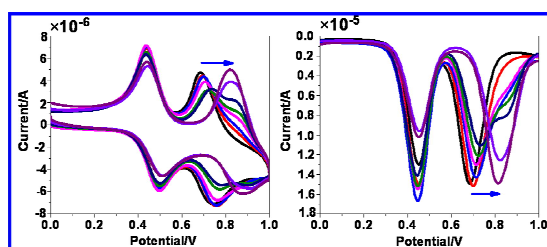


Fig. 8 Evolution of the CV (left) and DPV (right) of **1** (2.0×10^{-4} M) in CH_2Cl_2 when Pb^{2+} is added: from 0 to 1 equiv on a conventional three-electrode configuration, glassy carbon as the working electrode, platinum electrode as counter electrode, Ag/AgCl (3.0 M KCl) as reference electrode and 0.1 M $[(n\text{-Bu})_4\text{N}]\text{ClO}_4$ as supporting electrolyte at room temperature (scan rate: 100 mV/s).

CV and DPV for receptor **1** and complex $\mathbf{1}\cdot\text{Pb}^{2+}$ towards HSO_4^- (from 0 to 10 equiv.) were also conducted. Changes achieved maxima when 4 equiv. of HSO_4^- was added to the CH_2Cl_2 solutions of receptor **1**. As shown in Fig. S16, the two reduction peaks had cathodic shifts of 80 mV and 63 mV for Fc1 unit and Fc2 unit, respectively, while the oxidation peak was a small cathodic shift of 25 mV for Fc2 unit only. The electrochemical behaviors for complex $\mathbf{1}\cdot\text{Pb}^{2+}$ towards HSO_4^- showed that small anodic shifts of 29 mV and 25 mV were observed on the oxidation peak and the reduction peak of Fc2 unit when 2 equiv. HSO_4^- was added, respectively. However, with the increase of HSO_4^- , the CV behavior had been changing, intriguingly when the increment of HSO_4^- was 10 equivalents, varying degree of cathodic shifts on the two redox waves were occurred (Fig. S17). From the above discussions, we can see that the electrochemical behaviors of the receptor **1** containing HSO_4^- had a distinct response compared with that of involving Pb^{2+} .

2.3. Binding modes of receptor **1** for Pb^{2+} and HSO_4^-

In order to seek more detailed information of the binding modes in these recognition processes, ^1H NMR experiments were investigated. However, when CD_3CN solutions were used as the solvent solubility problems were encountered, thus the NMR experiments were studied in CDCl_3 solutions. In view of this, fluorescence spectra of **1** toward Pb^{2+} and HSO_4^- in CHCl_3 were performed (Fig S18) and the result displayed absolutely no significant change compared with that in CH_3CN . As shown in Fig. 9, upon addition of Pb^{2+} (1.0 equiv.) to the solution of **1**, the pyridine ring protons (H2, H3) are downshifted by 0.14 ppm and 0.27 ppm respectively, thus H1 is upshifted by 0.12 ppm and moved into a multi peak together with H3. H_α and H_β protons of the mono-substituted Cp adjacent to the imidazole ring are also downshifted by 0.20-0.30 ppm. However, addition of the HSO_4^- anion (1 equiv.) to receptor **1** induced an appreciable upshift by 0.25 ppm and 0.13 ppm for the H1 and H2 protons, respectively, H_β protons are also upshifted by 0.14 ppm whereas H_α protons are downshifted by 0.02 ppm. The different displacement of H_α protons distinguished from other protons illustrated that H_α protons involved in hydrogen binding. Job's plot (Fig S19) indicated a 1:1 binding stoichiometry for complexes $\mathbf{1}\cdot\text{HSO}_4^-$ and the association constant was calculated to be $K_a = 6.32 \times 10^3 \text{ M}^{-1}$. Likewise, addition of 1 equiv. Pb^{2+} and 1 equiv. HSO_4^- to receptor **1** gave rise to a comprehensive change of not only pyridine ring protons but also ferrocenyl protons compared with that towards Pb^{2+} or HSO_4^- only (Fig. 9). Evolution of the H2 proton monitored by ^1H NMR titration revealed that Pb^{2+} and HSO_4^- were coordinated to different binding sites of receptor **1**, respectively (Fig. S20). Furthermore, ^1H NMR experiments of complex $\mathbf{1}\cdot\text{Pb}^{2+}$ toward F^- were performed and analyzed quantitatively (Fig. S21). The NMR shift changes of F^- towards complex $\mathbf{1}\cdot\text{Pb}^{2+}$ can prove once again that anions X ($\text{X} = \text{F}^-, \text{Cl}^-, \text{Br}^-, \text{I}^-, \text{AcO}^-, \text{H}_2\text{PO}_4^-$ and OH^-) dissociated the complex $\mathbf{1}\cdot\text{Pb}^{2+}$ to $\text{Pb}(\text{X})_2$ and free receptor **1**.

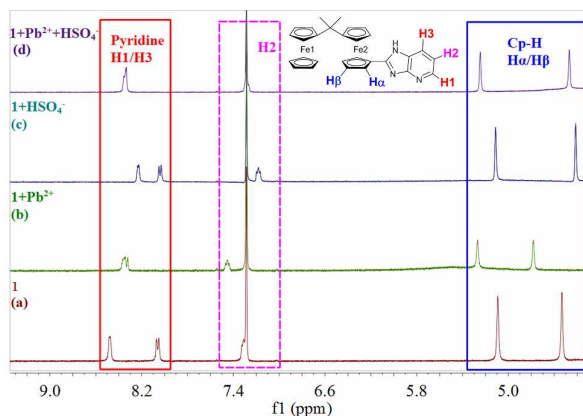


Fig. 9 ^1H NMR spectra of **1** ($9.45 \times 10^{-3} \text{ M}$) in CDCl_3 (a), after addition of 1 equiv. of $\text{Pb}(\text{ClO}_4)_2$ (b), 1 equiv. of $[(n\text{-Bu}_4\text{N})]\text{HSO}_4$ (c), 1 equiv. of $[(n\text{-Bu}_4\text{N})]\text{HSO}_4$ and 1 equiv. of $\text{Pb}(\text{ClO}_4)_2$ (d).

According to the above discussions, intermolecular hydrogen bonds between the receptor **1** and a solvent molecule DMSO $\text{N1-H32}\cdots\text{O}$ ($d_{\text{NH}\cdots\text{O}} = 1.80 \text{ \AA}$) and $\text{C22-H22}\cdots\text{O}$ ($d_{\text{CH}\cdots\text{O}} = 2.45 \text{ \AA}$) are responsible for the proposed mechanism of receptor **1** towards HSO_4^- , thus we proposed the plausible structure of the complex for **1** towards Pb^{2+} and HSO_4^- (Fig. 10).

This result has also been confirmed by ESI-MS, where a peak at m/z 879.01 corresponding to the complex $[1 \cdot \text{Pb}^{2+} \cdot \text{HSO}_4^- \cdot \text{HCO}_2\text{H}]$ is observed (HCO_2H was the residue mobile phase, Fig. S22).

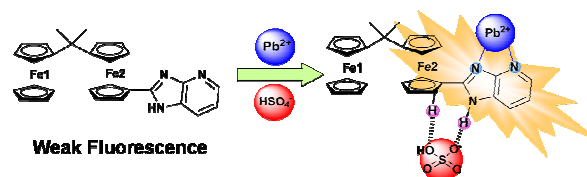


Fig. 10 Proposed sensing mechanism for receptor **1** towards Pb^{2+} and HSO_4^- .

2.4. Theoretical calculations

In order to explain the electronic spectra above-mentioned, theoretical calculation for the geometrical optimization of receptor **1** and complex $1 \cdot \text{Pb}^{2+}$ was performed at the density functional theory (DFT) level using the B3LYP hybrid functional. The 6-31G and 6-31G(d) basis sets were employed for H and C atoms, aug-cc-pVTZ for N atom and LANL2DZ with effective core potential for Fe and Pb atom, respectively. After obtaining the optimized structure, the further time-dependent density functional theory (TD-DFT) calculation was performed to investigate the excited states of receptor **1**. All calculations were performed using the Gaussian 09 package.⁴⁸ As shown in Fig. S23, the HOMO orbital is located completely on the Fc1 unit of **1** while the LUMO orbital is located almost on the heterocyclic ring system. A low intensity broad band at 451 nm in UV-vis absorption spectrum of **1** has a major contribution from the ferrocene based HOMO-3 \rightarrow LUMO+1 transition as deduced from the Gaussian, which is assigned as a $\text{Fe}^{2+} \rightarrow \text{Cp}$ transition. Further, the strong absorption band at 311 nm has the main contribution from the HOMO-2 \rightarrow LUMO transition, with relatively little contribution from the HOMO-2 \rightarrow LUMO+2 transition. Weak-emissive of receptor **1** may attributes to either electron transfer or energy transfer from the DFP group that act as an electron-donor, to the excited state of the heterocyclic ring system, acting as an electron-acceptor unit. It can be seen that the weak emissive of **1** is attributed to the rich electronic properties of DFP quenching the emission of fluorophore via PET. When Pb^{2+} is coordinated to the receptor **1**, HOMO and LUMO states of $1 \cdot \text{Pb}^{2+}$ are located mainly on the Pb^{2+} as well as Fc1 unit, which leads to its smaller HOMO \rightarrow LUMO gap. The smaller HOMO \rightarrow LUMO gap of complex $1 \cdot \text{Pb}^{2+}$ is more conducive to electronic transitions so that leading to fluorescence emission.

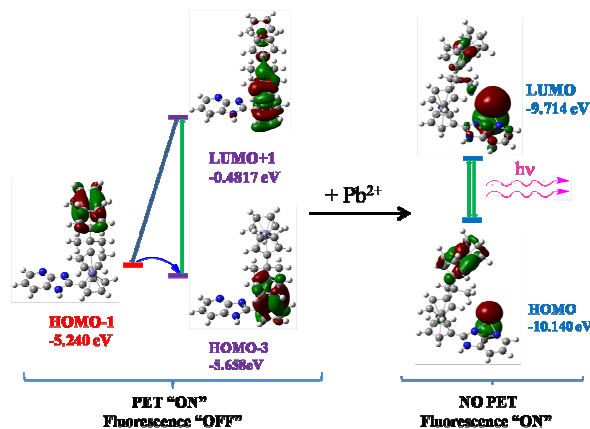


Fig. 11 HOMO–LUMO energy levels of **1** and its complex form with Pb^{2+} .

3. Conclusions

In conclusion, we demonstrated a Pb^{2+} and HSO_4^- concurrently responsive ion pair receptor **1** based on DFP, which was integrated with 1-deazapurine unit as the cation and anion binding sites. The structure of **1** was detected by single-crystal X-ray diffraction, and interestingly the intermolecular hydrogen bonds between receptor **1** and solvent molecule DMSO reflected the way HSO_4^- bond to **1**. Receptor **1** showed excellent selectivity and sensitivity for recognizing Pb^{2+} and HSO_4^- concurrently, accompanying significant fluorescence enhancement (more than 42-fold), obvious color change and apparent redox anodic/cathodic shift. The remarkable responses and selectivity exhibited by the ion pair receptor **1** illustrated that it could be used as a naked-eyes-detectable Pb^{2+} and HSO_4^- concurrently responsive chemosensor for applications in the surroundings. The 1:1 coordination modes of the receptor **1** towards Pb^{2+} or HSO_4^- were proposed based on Job's plot. Furthermore, according to the results of ^1H NMR titration and density functional theory, we proposed that the sensing mechanism as based on photo-induced electron transfer (PET). Additionally, further investigations on DFP-based ion pair receptors and towards enhancing their selectivity and sensitivity are currently ongoing in our laboratory.

Acknowledgment

We are grateful for the financial support from the National Natural Science Foundation of China (No. 21172036 and 21372043).

Notes and References

^a Department of Chemistry, Fuzhou University, Fuzhou 350116, China

^b State Key Laboratory of Photocatalysis on Energy and Environment, Fuzhou University, Fuzhou 350002, China

*Corresponding author. Tel./Fax: +86-591-22866161; E-mail: LCX395314748@163.com (C.-X. Lin).

**Corresponding author. Tel./Fax: +86-591-22866161; E-mail: yaofeng_yuan@fzu.edu.cn (Y.-F. Yuan).

†Electronic supplementary information (ESI) available: Materials and instruments, Synthesis details, Characteristic data and Supplementary spectra data, Fig. S1–S23, Tables S1–S4. CCDC 981227. See DOI: 10.1039/x0xx00000x

- [1] A. P. de Silva, G. D. McClean, S. Pagliari, *Chem. Commun.*, **2003**, 16, 2010-2011.
- [2] P. Molina, A. Tárraga, M. Alfonso, *Dalton Trans.*, **2014**, 43, 18-29.
- [3] E. Brunetti, J. F. Picron, K. Flidrova, G. Bruylants, K. Bartik, I. Jabin, *J. Org. Chem.*, **2014**, 79, 6179-6188.
- [4] R. Gotor, A. M. Costero, S. Gil, P. Gaviña, K. Rurack, *Eur. J. Org. Chem.*, **2014**, 2014, 4005-4013.
- [5] M. D. Gonzalez, F. Otón, R. A. Orenes, A. Espinosa, A. Tárraga, P. Molina, *Organometallics.*, **2014**, 33, 2837-2852.
- [6] A. J. McConnell, P. D. Beer, *Angew. Chem. Int. Edit.*, **2012**, 51, 5052-5061.
- [7] Q. C. Cinthia, G. M. Horacio, J. Carolina, D. L. F. Julio, *J. Incl. Phenom. Macrocycl. Chem.*, **2014**, 79, 161-169.
- [8] S. K. Kim, J. L. Sessler, *Acc. Chem. Res.*, **2014**, 47, 2525-2536.
- [9] I. Saha, K. H. Park, M. Han, S. K. Kim, V. M. Lynch, J. L. Sessler, C. H. Lee, *Org. Lett.*, **2014**, 16, 5414-5417.
- [10] F. Otón, A. Espinosa, A. Tárraga, I. Ratera, K. Wurst, J. Veciana, P. Molina, *Inorg. Chem.*, **2009**, 48, 1566-1576.
- [11] J. Hu, L. Chen, J. Shen, J. Luo, P. Deng, Y. Ren, H. Zeng, W. Feng, L. Yuan, *Chem. Commun.*, **2014**, 50, 8024-8027.
- [12] E. N. W. Howe, M. Bhadbhade, P. Thordarson, *J. Am. Chem. Soc.*, **2014**, 136, 7505-7516.
- [13] M. Alfonso, A. Tárraga, P. Molina, *Org. Lett.*, **2011**, 13, 6432-6435.
- [14] M. Alfonso, A. Tárraga, P. Molina, *J. Org. Chem.*, **2011**, 76, 939-947.
- [15] M. Alfonso, A. Tárraga, P. Molina, *Inorg. Chem.*, **2013**, 52, 7487-7496.
- [16] S. Das, S. Karmakar, S. Mardanya, S. Baitalik, *Dalton Trans.*, **2014**, 43, 3767-3782.
- [17] C. Bhaumik, D. Maity, S. Das, S. Baitalik, *RSC Adv.*, **2012**, 2, 2581-2594.
- [18] C. Bhaumik, S. Das, D. Maity, S. Baitalik, *Dalton Trans.*, **2011**, 40, 11795-11808.
- [19] M. Alfonso, A. Espinosa, A. Tárraga, P. Molina, *Org. Lett.*, **2011**, 13, 2078-2081.
- [20] R. Sun, L. Wang, H. Yu, Z. Abidin, Y. Chen, J. Huang, R. Tong, *Organometallics.*, **2014**, 33, 4560-4573.
- [21] A. Thakur, S. Ghosh, *Organometallics.*, **2012**, 31, 819-826.
- [22] M. Kaur, P. Kaur, V. Dhuna, S. Singh, K. Singh, *Dalton Trans.*, **2014**, 43, 5707-5712.
- [23] F. Otón, A. Tárraga, A. Espinosa, M. D. Velasco, P. Molina, *J. Org. Chem.*, **2006**, 71, 4590-4598.
- [24] M. Alfonso, J. Contreras-Garcia, A. Espinosa, A. Tárraga, P. Molina, *Dalton Trans.*, **2012**, 41, 4437-4444.
- [25] M. Alfonso, A. Sola, A. Caballero, A. Tárraga, P. Molina, *Dalton Trans.*, **2009**, 9653-9658.
- [26] F. Zapata, A. Caballero, A. Espinosa, A. Tárraga, P. Molina, *Org. Lett.*, **2007**, 10, 41-44.
- [27] M. Alfonso, A. Espinosa, A. Tárraga, P. Molina, *Chem. Commun.*, **2012**, 48, 6848-6850.
- [28] T. Romero, R. A. Orenes, A. Tárraga, P. Molina, *Organometallics.*, **2013**, 32, 5740-5753.
- [29] M. Alfonso, A. Tárraga, P. Molina, *Inorg. Chem.*, **2013**, 52, 7487-7496.
- [30] F. Zapata, A. Caballero, A. Espinosa, A. Tárraga, P. Molina, *Dalton Trans.*, **2010**, 39, 5429-5431.
- [31] B. Wei, Y. Gao, C. X. Lin, H. D. Li, L. L. Xie, Y. F. Yuan, *J. Organomet. Chem.*, **2011**, 696, 1574-1578.
- [32] R. J. Xie, L. M. Han, Q. L. Suo, H. L. Hong, M. H. Luo, *J. Coord. Chem.*, **2010**, 63, 1700-1710.
- [33] Q. L. Suo, L. M. Han, Y. B. Wang, J. H. Ye, N. Zhu, X. B. Leng, J. Sun, *J. Coord. Chem.*, **2004**, 57, 17-18.
- [34] Z. M. Su, H. M. Ye, X. X. Zhu, L. L. Xie, S. Bai, Y. F. Yuan, *J. Organomet. Chem.*, **2014**, 750, 162-168.
- [35] M. R. Ajayakumar, G. Hundal, P. Mukhopadhyay, *Chem. Commun.*, **2013**, 49, 7684-7686.
- [36] M. R. Ajayakumar, P. Mukhopadhyay, S. Yadav, S. Ghosh, *Org. Lett.*, **2010**, 12, 2646-2649.
- [37] M. R. Ajayakumar, D. Asthana, P. Mukhopadhyay, *Org. Lett.*, **2012**, 14, 4822-4825.
- [38] T. Klimova, E. I. Klimova, M. Martínez García, J. M. Méndez Stivalet, L. Ruíz Ramírez, *J. Organomet. Chem.*, **2001**, 633, 137-142.
- [39] J. R. Lakowicz, *Principles of Fluorescence Spectroscopy*, 3rd ed. Springer-Verla, Berlin, **2006**, p9.
- [40] M. Emrullahoğlu, M. Üçüncü, E. Karakus, *Chem. Commun.*, **2013**, 49, 7836.
- [41] M. Isik, T. Ozdemir, I. S. Turan, S. Kolemen, E. U. Akkaya, *Org. Lett.*, **2013**, 15, 216.

- [42] Guidelines for drinking water quality, 2nd ed.; World Health Organization: Geneva, 1996; Vol. 2, p 940.
- [43] P. Thordarson, *Chem. Soc. Rev.*, **2011**, *40*, 1305–1323.
- [44] Q. X. Liu, Z. Q. Yao, X. J. Zhao, A. H. Chen, X. Q. Yang, S. W. Liu, X. G. Wang, *Organometallics.*, **2011**, *30*, 3732–3739.
- [45] F. Zapata, A. Caballero, A. Tárraga, P. Molina, *J. Org. Chem.*, **2009**, *75*, 162-169.
- [46] K. Q. Wu, J. G. Jian, J. F. Yan, L. L. Xie, F. B. Xu, S. Bai, P. Nockemann, Y. F. Yuan, *Organometallics.*, **2011**, *30*, 3504–3511.
- [47] M. S. Rodriguez-Morgade, M. Planells, T. Torres, P. Ballester, E. Palomares, *J. Mater. Chem.*, **2008**, *18*, 176-181.
- [48] Frisch, M. J.; et al. *Gaussian 09*, revision A.02; Gaussian, Inc.: Wallingford, CT, **2009**.